

1 **SKS splitting in Southern Italy: anisotropy variations in a fragmented subduction**
2 **zone.**

3

4 **Baccheschi P.^{1,*}, Margheriti L.², Steckler M. S.³ and CAT/SCAN seismology team †**

5

6 ¹ Istituto Nazionale di Geofisica e Vulcanologia, CNT, Grottaminarda, Italy

7 ² Istituto Nazionale di Geofisica e Vulcanologia, CNT, Roma, Italy

8 ³ Lamont-Doherty Earth Observatory, Palisades, NY 10964, USA

9 † L. Abruzzese, A. Amato, J Armbruster, F. Di Luccio, A. Gervasi, I. Guerra, A.

10 Lerner-Lam, P. Persaud. and L. Seeber.

11

12 **Abstract**

13 In this paper we present a collection of good quality shear wave splitting measurements
14 in Southern Italy. In addition to a large amount of previous splitting measurements, we
15 present new data from 15 teleseisms recorded from 2003 to 2006 at the 40 stations of the
16 CAT/SCAN temporary network. These new measurements provide additional
17 constraints on the anisotropic behaviour of the study region and better define the fast
18 directions in the southern part of the Apulian Platform. For our analysis we have
19 selected well-recorded SKS phases and we have used the method of Silver and Chan to
20 obtain the splitting parameters: the azimuth of the fast polarized shear wave (ϕ) and

*Corresponding author. Istituto Nazionale di Geofisica e Vulcanologia, Via di Vigna Murata, 605 – 00143
Rome, Italy. Tel: +39 06 51860619; fax +39 06 51860507.

E-mail address: baccheschi@ingv.it.

21 delay time (δt). Shear wave splitting results reveal the presence of a strong seismic
22 anisotropy in the subduction system below the region. Three different geological and
23 geodynamic regions are characterized by different anisotropic parameters. The Calabrian
24 Arc domain has fast directions oriented NNE-SSW and the Southern Apennines domain
25 has fast directions oriented NNW-SSE. This rotation of fast axes, following the arcuate
26 shape of the slab, is marked by a lack of resolved measurements which occurs at the
27 transition zone between those two domains. The third domain is identified in the
28 Apulian Platform: here fast directions are oriented almost N-S in the northern part and
29 NNE-SSW to ENE-WSW in the southern one. The large number of splitting parameters
30 evaluated for events coming from different back-azimuth allows us to hypothesize the
31 presence of a depth-dependent anisotropic structure which should be more complicated
32 than a simple 2 layer model below the Southern Apennines and the Calabrian Arc
33 domains and to constrain at 50 km depth the upper limit of the anisotropic layer, at least
34 at the edge of Southern Apennines and Apulian Platform. We interpret the variability in
35 fast directions as related to the fragmented subduction system in the mantle of this
36 region. The trench-parallel ϕ observed in Calabrian Arc and in Southern Apennines has
37 its main source in the asthenospheric flow below the slab likely due to the pressure
38 induced by the retrograde motion of the slab itself. The pattern of ϕ in the Apulian
39 Platform does not appear to be the direct result of the rollback motion of the slab, whose
40 influence is limited to about 100 km from the slab. The anisotropy in the Apulian
41 Platform may be related to an asthenospheric flow deflected by the complicated structure
42 of the Adriatic microplate or may also be explained as frozen-in lithospheric anisotropy.

43

44 **Keywords:** Shear wave splitting; subduction; mantle flow; Southern Italy

45 **Introduction**

46 Crystals and most common materials are intrinsically anisotropic, with seismic wave
47 velocities varying for different propagation and polarization direction. The knowledge
48 of the anisotropic behavior of the mantle is an important tool in deep earth studies as it
49 is an indicator of mineral orientation and thus mantle flow. Anisotropy has been used to
50 discuss whether plate tectonics is driven from below by mantle flow or from above by
51 plates (*Silver and Holt, 2002*). It aids in investigations of the relationship between plate
52 motions, mantle flow at depth and the tectonic deformation. In recent years, numerous
53 studies have been carried out to characterize the strain pattern of the mantle. Studies of
54 mantle deformation are particularly focused on the anisotropic behaviour of the upper
55 mantle and there is a growing number of anisotropic studies in active tectonic regions,
56 such as subduction zones (*Ando et al., 1983; Fischer and Yang, 1994; Russo and Silver,*
57 *1994; Fouch and Fischer, 1996; Fischer et al., 1998; Savage, 1999; Peyton et al. 2001;*
58 *Hatzfeld et al. 2001, Park and Levin, 2002*). It is widely accepted that in the upper
59 mantle, the most likely mechanism that generates seismic anisotropy is lattice preferred
60 orientation (LPO) of the anisotropic olivine crystals. The alignment of the olivine
61 crystals in the mantle flow direction and the direct relationship between splitting
62 parameters and the crystallographic fabric of the mantle make the subduction zones one
63 of the best places to map the mantle deformation and to constrain the interaction
64 between the rigid subducting plate and the ductile mantle. Several studies show that
65 subduction zones exhibit a broad range of splitting directions. Many convergent margin
66 zones are characterized by arc-parallel fast directions, as in the Tonga (*Fischer and*
67 *Wiens, 1996*) and in the Mariana subduction zones (*Fouch and Fischer, 1998; Pozgay et*
68 *al., 2007*). Trench-sub-parallel fast directions are found in New Zealand (*Audoine et*

69 *al.*, 2000), in the Ryukyu arc (*Long and van der Hilst, 2006*), in Japan (*Long and van*
70 *der Hilst, 2005*) and South America (*Polet et al., 2000*). Other subduction zones exhibit
71 both trench-perpendicular and trench-parallel fast directions, as in Lau back-arc (*Smith*
72 *et al., 2001*) and Kamchatka (*Peyton et al., 2001*). This variable pattern of shear wave
73 polarization direction can be explained considering the large and extremely different
74 factors which affect and complicate the anisotropy, such as the influence of water on
75 olivine deformation (*Jung and Karato, 2001*), effects of dynamic recrystallization
76 (*Kaminski and Ribe, 2001*), strain partitioning between melt-poor and melt-rich regions
77 (*Holtzman et al., 2003, Kaminski, 2006*), local scale flow in the mantle wedge induced
78 by the subducting plate motion (*Vinnik and Kind, 1993; Gledhill and Gubbins, 1996*),
79 and frozen lithospheric anisotropy in the slab (*Plomerova et al., 2006*). Moreover, the
80 presence of slab edges, their geometry, tears in the slab and discontinuities may further
81 complicate the flow pattern (*i.e., Peyton et al., 2001*).

82 In this study, we have analyzed a large number of events increasing the number of
83 splitting measurements for Southern Italy. This has allowed us to better reveal the
84 variations in the anisotropic parameters between three different geological and
85 anisotropic domains: the highly deformed Southern Apennines and Calabrian Arc
86 mountain belts and the weakly deformed Apulia Platform. Also, new evidence of
87 anisotropy in the southernmost part of the Apulian Platform are found.

88 We describe the range of splitting behaviour over the study region. There are areas
89 where splitting patterns are generally consistent with a simple anisotropic model, and
90 other places where we see evidence for complexity in the anisotropic fabric. We try to
91 relate these differences to tectonic features and to the upper mantle structure.

92

93 ***1.1 Geodynamics of the Calabrian Arc Subduction System***

94 The Tyrrhenian Sea-Calabrian Arc System (Fig. 1) is part of the complex tectonic
95 boundary between the Africa-Eurasia macroplates. The slow N-S convergent motion
96 between these two major plates has always been invoked as the primary tectonic process
97 in the Mediterranean area (*Wortel and Spackman, 2000*). Nevertheless, the existence of
98 large basins with E-W extensional tectonics, such as the Tyrrhenian Sea, along with
99 compressional arcuate mountain belts, such as the Apennines and Alps, imply the
100 existence of forces and processes independent of the Africa-Eurasia collision (*Dewey et*
101 *al., 1989; Jolivet and Faccenna, 2000*). Moreover, the rate of convergence between
102 these two plates is on the order of 1-2 cm/yr (*Faccenna et al., 2004*), which is far slower
103 than the rate (5-7 cm/yr) of both the opening of the Tyrrhenian back-arc basin and of the
104 building of the Apenninic and Calabrian mountains (*Malinverno and Ryan, 1986;*
105 *Patacca et al., 1990*). Numerous authors (i.e., *Gueguen et al, 1998; Carminati et al,*
106 *1998; Faccenna et al. 2001, 2003, 2004, 2005*) explain the geodynamic setting of the
107 Tyrrhenian Sea-Calabrian Arc System as resulting from the southeast retrograde motion
108 of the northwestward subducting Western Mediterranean slab and the associated arc
109 migration. The rollback of the slab provided the driving force for the creation of the
110 backarc, extensional Tyrrhenian Sea and building of the Southern Apennines and
111 Calabrian arcuate orogenic belts.

112 The development of the present Tyrrhenian Sea - Calabrian Arc has been inherited from
113 several phases of fragmentation of the Western Mediterranean subduction zone. At
114 present, subduction may be active only in the Ionian area, beneath the Calabrian Arc,
115 while a young slab window develops at the Southern Apennines (*Lucente and Speranza,*
116 *2001; Faccenna et al., 2003, 2005*).

117 Beneath the Calabrian Arc are many geophysical features that suggest the presence of
118 subducted oceanic Ionian lithosphere. The actual existence of the slab is defined by the
119 occurrence of many shallow and deep earthquakes concentrated along the Calabrian Arc
120 and in the southeastern sector of the Tyrrhenian basin respectively (Fig. 2a) (*Selvaggi*
121 *and Chiarabba, 1995; Chiarabba et al., 2005*). The distribution of earthquakes in
122 vertical sections (Fig. 2b) depicts the Calabrian slab extending from the Ionian foreland
123 in front of the Calabrian Arc to the central sector of the Tyrrhenian backarc basin (Fig.
124 2a,b). At shallow depth, the seismicity images a sub-horizontal seismic plane that could
125 be interpreted as the upper portion of the subducting Ionian lithosphere (*Frepoli et al.,*
126 *1996; Selvaggi 2001; Chiarabba et al., 2005; Pondrelli et al., 2004*). Beneath the
127 northern sector of the Calabrian Arc, the slab has a gap between 100 and 200 km depth,
128 but forms continuous body at greater depth. The lateral extent of this slab, as delineated
129 by seismicity and tomography, is very narrow, no wider than 250 km. Several seismic
130 tomography studies (*Piromallo and Morelli, 2003; Wortel and Spakman, 1993; Cimini,*
131 *1999; Lucente et al., 1999; Montuori et al., 2007*) describe the present-day shape and
132 extent of the slab beyond where it is imaged by seismicity (Fig. 3). The studies agree on
133 several features. A vertical section (Fig 3) reveals that at 100 km depth a high velocity
134 anomaly is present only where the deep seismicity is located. At the same depth, the
135 adjacent Tyrrhenian Sea, Sicily, the Southern Apennines and the Adriatic Sea are
136 characterized by low velocity anomalies. At greater depth, the fast velocity anomaly
137 broadens its size lying beneath the whole Calabrian Arc. At about 300km depth, the high
138 velocity anomaly is a continuous body running from the Southern Apennines in the NE
139 to the Sicily-Maghrebides in the SW, and extending from the Calabrian Arc to SE sector
140 of the Tyrrhenian Sea. This high velocity anomaly is interpreted as the sinking slab

141 (*Piromallo and Morelli, 2003*). Thus, the slab is horizontal in its shallow portion on the
142 Ionian side, it is steeply dipping (about 70°) to NW down to 400 km and then it bends
143 towards horizontal in the transition zone, lying flat on the upper mantle-lower mantle
144 boundary (660 km) (*Lucente et al., 1999; Piromallo and Morelli, 2003*).

145 Geodetic data show that today the Calabrian Arc is not retreating and that back-arc
146 extension is not active (*Hollenstein et al, 2003; D'Agostino and Selvaggi, 2004*);
147 however, Nicolosi et al. (*2006*) by unraveling magnetic anomalies in the young
148 Tyrrhenian Sea oceanic crust, suggest that back arc spreading was always episodic.

149

150 ***1.2 Geological features of the Southern Italy***

151 The surface tectonics of the area analyzed in this study (Fig. 1) can be described by three
152 main regions: the Calabrian Arc, the Southern Apennines and the Apulia Platform. The
153 Calabrian Arc fold and thrust belt is part of the accretionary wedge resulting from the
154 sinking of the old oceanic crust still present below the Ionian Sea. The top of the thrust
155 stack in the Calabrian Arc is composed of metamorphic basement slices. These exposed
156 Paleozoic crystalline rocks suggest that this part of Calabrian Arc is a remnant of the
157 Europe-Iberia plate (*Rossetti et al., 2004*) that migrated southward with the subduction
158 system (*Gueguen et al., 1998*).

159 A different structural style defines the Southern Apennines fold and thrust belt, resulted
160 from the sinking of the Ionian lithosphere and from the collision with the Adriatic
161 microplate (*Patacca and Scandone, 1989*). It was constructed by the imbrications of a
162 succession of carbonate platforms and pelagic basins domains. The most external of
163 these domains is the Apulia Platform which, along with the underlying basement, is
164 partly involved in the orogenic wedge and partly forms the foreland lying below the

165 outer front of the Apenninic chain (*Patacca et al., 2000*). The Apulian Platform is part
166 of the Adriatic microplate considered by some authors as an African promontory
167 (*Rosenbaum and Lister, 2004*) and by others (*Battaglia et al. 2004*) as an independent
168 microplate. The Adriatic microplate subducted below the Eurasian plate between the
169 Cretaceous and the Tertiary forming the SW-vergent Dinarides (*Aubouin et al., 1972*)
170 and, during the Tertiary, the NE-vergent Apennines.

171

172 ***1.3 Previous studies of anisotropy in the region***

173 Previous SKS splitting studies in the western Mediterranean subduction zone (*Barruol*
174 *and Granet, 2002; Margheriti et al., 2003; Civello and Margheriti, 2004; Schimid et al.,*
175 *2004; Barruol et al 2004; Lucente et al., 2006, Plomerova et al. 2006; Baccheschi et al.*
176 *2007; Salimbeni et al. 2007*) found quite large delay times and relate the trench-
177 perpendicular fast directions in the mantle wedge and trench-parallel fast direction
178 along the trench itself to the retrograde motion of the retreating slab (*Buttles and Olson,*
179 *1998*). In addition, some complications associated with the Aeolian volcanic arc have
180 been found. Civello and Margheriti (*2004*) interpreted the trench-perpendicular fast
181 direction around the western edge of the present-day Calabrian slab, beneath the Sicily
182 Channel, as a return flow caused by the rollback of the narrow retreating slab. Similar
183 toroidal mantle flow had been modelled by Kincaid & Griffiths (*2003*). In Baccheschi et
184 al. (*2007*), such trench-perpendicular fast directions were not found at the NE edge of
185 the slab beneath the Southern Apennines, where another slab tear is hypothesized by P-
186 waves tomographic models (*Piromallo and Morelli, 2003*). Baccheschi et al. (*2007*)
187 suggests that a possible return flow could be hypothesized at the boundary of the

188 Southern Apennines and Central Apennines. Moreover, they define that the influence of
189 the slab rollback in the sub-slab mantle is limited to less than 100 km from the slab.

190

191 **2 Data and methods**

192 When a shear wave passes through an anisotropic medium on its path to the receiver, it
193 splits into two pulses which travel at different speeds: these are denoted as the fast and
194 slow components and have polarization orientations normal to each other (*Vinnik and*
195 *Kind, 1993; Savage, 1999; Bowman and Ando, 1987*). The splitting parameters used to
196 describe an anisotropic medium are the polarization azimuth of the fast shear wave, φ ,
197 (the preferred orientation of the anisotropic crystals), and the delay time, δt , between the
198 fast and slow wave arrivals, which is a measure of the thickness and of the strength of
199 the anisotropic layer. To obtain the shear-wave polarization azimuth and delay time, we
200 used the method described by Silver and Chan (1991), assuming that shear waves pass
201 through a medium with homogeneous anisotropy and with an horizontal fast axis. This
202 method is based on a grid search to find the pair of splitting parameters that best
203 minimize the energy on the transverse component. The splitting analysis on SKS phases
204 is simpler than for other phases. Due to SKS waves passing through the liquid core, all
205 source-side anisotropy is removed. The P-S conversion at the core-mantle boundary
206 provides a known polarization direction; they are polarized on the radial component.
207 Therefore, the presence of energy on the transverse component indicates that the SKS
208 waves have travelled through the anisotropic region on the receiver side (*Silver and*
209 *Chan, 1991*). Another advantage is that SKS is an isolated phase for epicentral distances
210 ranging between 86° and 106° (*Silver, 1996*).

211 We have calculated splitting parameters for 15 teleseisms (Fig. 4) with high signal to
212 noise ratios recorded from December 2003 to March 2006 at the 40 CAT/SCAN
213 (Calabrian-Apennine-Tyrrhenian/Subduction-Collision-Accretion Network) stations
214 (<http://www.ldeo.columbia.edu/res/pi/catscan>) (Fig. 5) .

215 We selected earthquakes with magnitude greater than 6.0 and epicentral distance Δ°
216 ranging from 87° to 112° . The earthquakes span all back-azimuth, but are primarily
217 concentrated in the E to NE and in the W (Fig. 4). To obtain the best signal to noise
218 ratio, all teleseisms are band-pass filtered with a Butterworth filter to frequencies
219 between 0.03-0.3 Hz. We considered as good measurements only the events with
220 waveforms that exhibit both SKS energy on the transverse component and elliptical
221 particle motion before anisotropy correction and, those, after the correction for
222 anisotropy, show a clear energy reduction on transverse component, rectilinear
223 polarization of the horizontal particle motions, and a good correlation between the fast
224 and slow waves. The final collection of splitting results includes also null measurements.
225 We considered as nulls those measurements in which the original seismograms do not
226 show energy on the transverse component. We did not include in the results complex
227 waveforms not resolvable by the splitting code to avoid the ambiguity between these two
228 different results (*Levin et al 2006*). A null direction does not necessarily mean that
229 anisotropy is absent beneath the station, but could also mean that the shear wave is
230 initially polarized parallel to either the fast or slow direction. This second possibility is
231 the most likely if null directions are obtained along with non-null measurements at the
232 same station. In Figure 6, we show an example of null measurement, an example of a
233 well-constrained result, and an example of complex waveform for which no results are
234 found.

235 **3 Results: geographical variations in splitting parameters**

236 The final collection consists of 185 new SKS high quality measurements, 43 of which
237 are nulls. For each event (Table 1) we report the complete list of individual shear wave
238 splitting parameters along with station and event parameters (Table 1 also includes
239 single measurements from *Civello and Margheriti, 2004* that were not published
240 elsewhere). Results are mapped in Figure 7 along with the splitting results obtained in
241 the previous studies (*Margheriti et al 2003; Civello and Margheriti, 2004; Lucente et al*
242 *2006; Baccheschi et al., 2007*) to get a general picture of the anisotropy in the region.
243 We analyze and discuss the new splitting parameters results together with the results
244 presented in *Baccheschi et al. (2007)*. At most of the stations used, we obtained both
245 null and non-null results. The delay time varies between 0.6 s and 3.0 s with an average
246 value of about 1.8 s. The value of δt is in agreement with the large delay time between
247 fast and slow components found by other authors in the Mediterranean region (*Schmid*
248 *et al., 2004; Salimbeni et al., this volume*) and in other subduction zones (*Audoine et al.,*
249 *2004; Anderson et al., 2004; Russo and Silver 1994*). Considering an average
250 anisotropy of about 5%, then a delay time of 1.8 s would correspond to an anisotropic
251 layer ~ 200 km thick (*Mainprice et al, 2000*). In subduction zone environments,
252 anisotropy has been inferred to exist at depths as great as 400 km or perhaps deeper
253 (*Fouch and Fischer, 1996; Fischer and Wiens, 1996*). We found the largest δt (up to 3.0
254 s) along the crest of the Southern Apennine chain and along the highest sector of the
255 Calabrian Arc.

256 It is evident that the orientation of ϕ is variable and changes moving from Calabrian Arc
257 to the Southern Apennines and to the Apulian Platform. A clear separation is present in
258 the transition zone between the Calabrian Arc and the Southern Apennines where not

259 only the fast polarization direction changes, but there is also a lack of measurements
260 that is not related to the absence of stations and therefore of data. At these stations
261 (black triangles in Fig. 5) 90% of the analyzed seismograms are either complex, and do
262 not give clear and simple splitting results (as the CIVI example in Fig. 6), or gave a null
263 measurements. The Calabrian Arc and Southern Apennines show a pattern of trench-
264 parallel fast axes. In the Calabrian Arc, fast directions are prevalently oriented NE-SW
265 parallel to the slab strike. Moving toward the Southern Apennines, especially on its
266 Tyrrhenian side, the fast directions rotate to follow the curved contour of the slab and
267 are oriented NNW-SSE. Toward the Apulian Platform the orientation of ϕ exhibits a
268 clear rotation from N-S in the northern sector to NNE-SSW toward the central-southern
269 sector. The splitting results in the southernmost sector of the Apulian Platform, with fast
270 directions oriented ENE-WSW, testify to the presence of an anisotropic mantle, whereas
271 previous studies (*Baccheschi et al., 2007*) identified only nulls. In each of the studied
272 regions, we have found some good measurements with orientation of fast directions that
273 differs from the prevalent trend. In the following paragraphs we try to investigate the
274 causes of the variability of the splitting parameters. We have separated the well-
275 constrained SKS measurements in three groups: the Calabrian Arc, the Southern
276 Apennines and the Apulia Platform; each of these corresponds to a region with a
277 different geological and geodynamic history. We have made frequency plots of ϕ for
278 each sector (Fig. 8), obtaining 121 measurements for the Southern Apennines, 118
279 measurements for the Calabrian Arc and 37 measurements for the Apulia Platform. The
280 rose diagrams show that the fast directions are quite stable in the Southern Apennines
281 and Calabrian Arc, showing a prevalent trench-parallel direction. This trend suggests
282 the existence of an anisotropic volume with uniform characteristics for each one. In the

283 Apulia Platform, fast directions are less homogeneous and might reflect a more
284 complicated anisotropic structure. The prevalent φ is N-S, but NNE-SSW and ENE-
285 WSW directions are also common. The N-S direction prevails in the northern sector of
286 the Apulia Platform, while the NNE-SSW and ENE-WSW φ are found farther south
287 together with several null measurements. The existence of regions each one with
288 uniform anisotropic pattern, suggest a lateral variation in anisotropic structure. Even if
289 we cannot exclude the existence of a volume with inclined fast axis, we prefer to
290 interpret the variation in anisotropic parameters in terms of lateral or vertical variation
291 of anisotropic volumes with horizontal fast axis following the initial hypothesis
292 corresponding to the Silver and Chan (1991) method used.

293

294 ***3.1. Splitting parameters variability versus back-azimuth***

295 In order to check for possible dependence between the back-azimuth and the anisotropic
296 parameters we have grouped the stations of each anisotropic domain and we plot fast
297 directions and delay times versus back-azimuths (Fig. 9). The results obtained in this
298 study are combined with the splitting measurements in Baccheschi et al. (2007).
299 Analysis of several events coming from different back-azimuth are needed to clarify the
300 complex fabric of the anisotropic structures at depth (Levin et al. 2006; Long and van
301 der Hilst, 2005). Consideration of the distributions of φ and δt versus the back-azimuth
302 on the diagrams (Fig. 9) should be viewed with caution since each plot includes a large
303 number of stations. We discuss the plots for the Southern Apennines and for the
304 Calabrian Arc, while for the Apulian platform the number of non-null measurements is
305 not sufficient for such analysis. In Southern Apennines and in Calabrian Arc the
306 measurements show a uniform pattern, suggesting that the anisotropic structure beneath

307 the stations should be quite homogeneous. It is interesting to note that the measures that
308 deviate from the most common fast direction are found for specific back-azimuth:
309 measurements in the Southern Apennines with back-azimuths of about 70° and 70°
310 $+180^\circ$ are much more scattered than the other measurements. In the Calabrian arc
311 measurements coming from back-azimuth of about 20° and $20^\circ+180^\circ$ have values
312 different from the most common. This may imply the presence of a layered anisotropic
313 structure beneath the stations (*Rumpker et al., 1999; Silver and Savage, 1994*). For each
314 of those two domains we have investigated the possible depth-dependent anisotropy by
315 computing a large number of two-layer models trying to fit the observed measurements
316 but none of the model fit the data sufficiently suggesting that the anisotropic structure in
317 the investigated regions is more complicated than a two-horizontal-layer model.

318

319 ***3.2. Splitting parameter variability along an E-W transect***

320 The pattern of SKS splitting for the Southern Italy show a change of the fast axes
321 orientation moving from the Southern Apennines to the Apulian Platform. To constrain
322 the position of where this change take place, we have displayed the value of φ and δt
323 along an E-W transect (Fig. 10) running from the Tyrrhenian Sea to the Adriatic Sea at
324 about latitude 40° (box AA' in Fig. 7). The fast axes rotate from NW in the Southern
325 Apennines to NE in the Apulian Platform. We observe two groups of fast directions;
326 one with values between -50° and 20° related to the Southern Apennines domain; the
327 other with values of φ between 30° and 70° related to the Apulia Platform domain. The
328 rotation of fast directions takes place almost at the surface tectonic boundary between
329 those different tectonic domains and corresponds to a distance along the profile of about
330 130 km. At stations located at this transition, NW-SE fast directions are found for

331 events coming from west and NE-SW fast directions are found for events coming from
332 east. This may imply the presence of a steep boundary between the two domains.

333

334 ***3.3. Lateral variation and depth of seismic anisotropy from Fresnel zones***

335 The variability of splitting parameters at the stations located near the boundary between
336 the Southern Apennines and the Apulia Platform for events coming from opposite back-
337 azimuths allows us to hypothesize the existence of a near vertical boundary between
338 these two anisotropic regions. If this assumption is correct and if we are in presence of
339 two anisotropic domains with horizontal fast axes, it is possible to give some constrains
340 on the depth of the anisotropic region. According to the method described by Alsina and
341 Sneider (1995), we have estimated the upper limit of the depth of the anisotropic region
342 by calculating the Fresnel zones. The size of the Fresnel zone at a given depth is given
343 by (Pearce and Mittleman; 2002):

$$Rf = \frac{1}{2} \sqrt{Tv h}$$

344

345 where Rf is the radius of the zones, T is the SKS dominant period (10 s), v is the wave
346 velocity (4.5 km/s from the IASP91 model) and h is the depth. Considering two
347 teleseismic events with opposite back-azimuth recorded at the same station and with
348 different splitting results, the anisotropic domain is estimated to be deeper than a certain
349 depth we note as Z_1 . Above Z_1 the rays travel through the same medium and the
350 corresponding Fresnel zones overlap. Below this depth the ray paths and Fresnel zones
351 for the two events are distinct, as shown by the difference in splitting parameters
352 observed for the two events. For our analysis we have used three stations (TRIC, ILCA
353 and CRAC) located along the transect at the transition zone between the Southern

354 Apennines and the Apulian Platform (Fig 11). At each of those stations, we have
355 analyzed two teleseisms with opposite back-azimuth, obtaining two different values of
356 fast directions. We have calculated the Fresnel zones at 50, 100, 150 and 200 km depth.
357 Our results show that the Fresnel zones partially overlap at a depth of 50 km, indicating
358 that above that depth they will be sampling roughly the same volume. In contrast, for
359 the other depths, the corresponding Fresnel zones are separated, indicating that the rays
360 sample different volumes below 50 km depth. These considerations allow us to suggest
361 that the main source of anisotropy is located below 50 km depth and that the primary
362 source is therefore not in the crust, at least at the transition zone between the Southern
363 Apennines and the Apulian Platform.

364

365 **4. Discussion**

366 The increased number and the close spacing of seismic stations installed in Southern
367 Italy in the framework of the CAT/SCAN and CESIS (Centro per la Sismologia e
368 l'Ingegneria Sismica) projects enabled us to collect a large number of shear wave
369 splitting measurements that has helped us to characterize the anisotropy distribution and
370 the mantle fabric of Southern Italy. The orientation of anisotropy can be altered by the
371 water (*Jung and Karato, 2001*). For systems with very little or no hydration, LPO of
372 olivine fast axes are aligned with the direction of flow in the dislocation creep regime
373 (*Zhang and Karato, 1995; Tommasi et al., 2000*). Experimental studies suggest that
374 olivine slip systems change under higher stress and hydration states (*Jung and Karato,*
375 *2001*). Since in subduction zones there are regions where these last conditions likely
376 exist, the development of olivine LPO may be significantly influenced by them
377 (*Kaminski et al. 2004*), especially in the forearc (*Kneller et al., 2005*). In this study,

378 such a volume corresponds to the offshore region in the Tyrrhenian Sea between
379 Calabria and the Aeolian Islands and, likely, is not sampled by the SKS rays analyzed.
380 Our SKS splittings are the results of anisotropy in the slab and subslab mantle and we
381 interpret them in terms of LPO of olivine due to strain associated with flow in the
382 asthenospheric mantle.

383

384 ***4.1. Is anisotropy related to lithospheric fabric or asthenospheric flow?***

385 The pattern of splitting parameters observed in this study seems to be consistent with a
386 primary source of the anisotropy localized into the asthenosphere. Most of the delay
387 time values are larger than 1.5 s. The average value is 1.8 s: if we consider an
388 anisotropy of about 5% (*Mainprice et al., 2000*), a δt of 1.8 s would correspond to a
389 thickness of the anisotropic layer of ~ 200 km. This implies that the main source of
390 anisotropy cannot be contained in the lithosphere, which is not thicker than 100 km in
391 the area (*Panza et al., 2007*). The Fresnel zone analysis seems to exclude the source of
392 shear wave splitting from being located in the upper 50 km, at least at the boundary
393 between Southern Apennines and Apulian Platform. Moreover, the presence of the slab
394 rollback is a reasonable cause of an active asthenospheric flow induced by the motion of
395 the slab and which we interpret as being responsible for most of the observed
396 anisotropy. In Southern Apennines and in Calabrian Arc, the observation of some back-
397 azimuthal dependence of fast directions and delay times allow us to hypothesize the
398 existence of vertical variations in anisotropy and also suggests a possible lithospheric
399 contribution to the anisotropy there.

400

401

402

403 **4.2. Possible pattern of asthenospheric flow**

404 If we interpret the anisotropic parameters in terms of asthenospheric flow, the trench-
405 parallel fast directions observed in Southern Apennines and in Calabrian Arc are likely
406 due to the pressure induced by retrograde motions of the slab (*Buttles and Olson, 1998*)
407 which induces the mantle to move horizontally around it creating a local-scale mantle
408 flow below the subducting plate. The slab acts as a barrier at depth, forcing the mantle
409 to flow parallel to its strike (*Russo and Silver, 1994*). Moving from south to north fast
410 axes rotate to follow the arcuate shape of the mountain chains and the curve of the
411 continuous Calabrian slab. Between the Calabrian Arc and the Southern Apennines we
412 see a great continuity in fast directions, but we also observe a lack both of null and non-
413 null measurements in the transition zone between these two different geological
414 domains. Geological models for the evolution of the Calabrian Arc include a left-lateral
415 offset between the Calabrian Arc and Southern Apennines of variable size (*Rosenbaum
416 and Lister, 2004; Faccenna et al., 2005*), which could result in a complex transition
417 zone characterized by incoherent anisotropic fabric in the mantle (*Plomerova et al.
418 2001*). Mantle flow may also be complicated by the presence of tears at the edges of the
419 Calabrian slab, as revealed by some tomographic images (*Piromallo and Morelli,
420 2003*). A tear in the slab may allow the mantle to flow through it, creating a return flow
421 from behind the subducting plate to the front of the slab (*Matcham et al., 2000*). Some
422 local studies of anisotropy (*Civello and Margheriti, 2004*) identify a mantle return flow
423 beneath the Sicily Channel through the tear at the SW edge of the Calabrian slab.
424 Baccheschi et al. (2007) did not find such a return flow also in the N-E edge of the same
425 slab, where tomographic models identify another tear. In this study we have added

426 measurements below the southern Apennines which show fast axes oriented prevalently
427 NNW-SSE. This confirm the idea that any existing tear is not wide enough to allow to
428 the mantle to flow horizontally through it (Fig. 12), or that the tear is too young to
429 reorganize the olivine structure (*Faccenna et al., 2005*). The delay times corresponding
430 to the slab parallel fast directions are very high (several measurements are higher than
431 2.0 s) suggesting that the mantle is deformed by the retrograde motion of the slab up to
432 a depth of about 300 km, where no tear is shown by tomographic images (Fig. 12).

433

434 ***4.3. Anisotropy in the subduction foreland***

435 Interesting results are observed in the Apulia. The main observation is the absence of
436 fast directions parallel to the strike of the slab. This different pattern of splitting
437 measurements could be related to previous geodynamic events frozen in the Apulian
438 Platform lithosphere and, more generally, in the Adriatic microplate. Fast axes are
439 oriented N-S in the northern sector, which show the same pattern of splitting
440 measurements found by previous studies (*Margheriti et al. 2003, Schmid et al., 2004*) in
441 the Adriatic microplate along the Italian Coast and along the Dalmatian Coast on the
442 western flank of the Dinarides mountains. In particular, in the easternmost sector of the
443 Northern Apennines not arc-parallel and oblique fast directions were found (*Plomerova*
444 *et al. 2006*).

445 Moving toward the southern sector of the Apulia Platform fast axes rotate and show a
446 prevalently NNE-SSW to ENE-WSW directions; in this sector most of the analyzed
447 waveforms return null measurements. This change in splitting parameters between the
448 northern and southern sector of the Apulia Platform is found around latitude 40°N
449 which could testify some past or current deep discontinuities inside the Adriatic

450 microplate. The orientations of fast directions found in the Apulia Platform are different
451 from to the ones observed in the adjacent Southern Apennines. This change takes place
452 almost at the surface tectonic boundary between those two different geological sectors.
453 If the flow beneath the Southern Apennines represents the zone of flow induced by the
454 rollback of the slab, then the edge of the zone where the flow is sufficiently strong to
455 have reoriented the mantle fabric is relatively sharp. The almost trench-perpendicular
456 splitting distributions in Apulia could be interpreted as a mantle flow not controlled by
457 the slab presence and geometry and not involved in the retrograde motion of the slab.
458 Together, these considerations suggest a very focused mantle flow below the slab and
459 that the presence and the rollback of the slab horizontally influence directly the mantle
460 deformation only in a limited zone (less than 100 km) close to the subducting plate. In
461 contrast, the observed seismic anisotropy properties in Apulian Platform could be
462 related to frozen-in fossil flow beneath the Adriatic microplate or to local
463 asthenospheric flow deflected by the roots of the Dinarides away from the orogen-
464 parallel direction. Moreover, the slightly lower values of δt and the abundance of nulls
465 in the weakly deformed Apulian foreland would suggest a possible lithospheric
466 contribution in this domain.

467

468 **5. Conclusion**

469 SKS splitting results collected in this study reveal the existence of strong and complex
470 seismic anisotropy beneath the Southern Italy. Numerous and closely spaced stations
471 allowed us to better constrain the anisotropic structure of the mantle. We observe
472 different fast axes orientations in three different tectonic and geological domains, each
473 one is characterized by relatively uniform anisotropic parameters. In the Southern

474 Apennines and in the Calabrian Arc fast axes show predominantly trench-parallel
475 orientation. The clear rotation, from south to north, of fast directions to be parallel to the
476 strike of the slab suggest that the anisotropy is closely controlled by subduction and by
477 the rollback motion of the slab. The combination of those two processes would be
478 responsible for activating mantle flow below and around the slab itself. The scarce
479 number of trench-perpendicular ϕ at the northernmost stations of the Southern
480 Apennines does not favour the hypothesis of a return flow around the NE edge of the
481 Calabrian slab through a slab gap in the Southern Apennines. We conclude that any slab
482 tear below the Southern Apennines is young and not wide enough to have allowed the
483 reorganization of mantle flow. We observe a large average delay time (1.8 s) especially
484 in Southern Apennines and in Calabrian Arc that seems to be consistent with the
485 primary source of anisotropy localized into the asthenosphere. Moreover, the
486 observations in Southern Apennines and in the Calabrian Arc of some back-azimuthal
487 variations lead us to consider the existence of depth-dependent anisotropy which should
488 be more complicated than a two-layer model. Moving from the Southern Apennines to
489 the adjacent Apulian Platform, our results show a change in the fast direction
490 orientations from trench-parallel to oblique with respect to the slab strike. This not
491 trench-parallel fast axes distribution reflects the pattern observed in the larger Adriatic
492 microplate, with fast directions ranging from N-S to NNE-SSW to ENE-WSW.
493 Therefore in this microplate the anisotropic fabric appears not to be controlled by
494 subduction geodynamics but could be related to a frozen-in lithospheric fossil flow or to
495 a local asthenospheric flow determined by the interaction between Calabrian slab
496 motion and the Dinarides roots.
497

498

499 **References**

500 Alsina, D., Snieder, R., 1995. Small-scale sublithospheric continental mantle
501 deformation: constraints from SKS splitting observations. *Geophys. J. Int.*, 123:
502 431-448.

503 Anderson, M. L., Zandt, G., Triep, E., Fouch, M., Beck, S., 2004. Anisotropy and
504 mantle flow in the Chile-Argentina subduction zone from shear wave splitting
505 analysis. *Geophys. Res. Lett.*, vol. 31, L23608. doi: 10.1029/2004GL020906.

506 Ando, M., Ishikawa, Y., Yamazaki, F., 1983. Shear wave polarization anisotropy in the
507 upper mantle beneath Honshu, Japan. *J. Geophys. Res.*, 88: 5850–5864.

508 Aubouin, J., Blanchet, R., Cadet, J-P, Celet, P., Charvet, J., Chorowicz, J., Cousin, M.,
509 Rampnoux, J-P., 1972. Essai sur la géologie des Dinarides. *Bull. Soc. Géol. Fr.*,
510 12: 1060-1095.

511 Audoine, E., Savage, M. K., 2004. Anisotropic structure under a back arc spreading
512 region, the Taupo Volcanic Zone, New Zealand. *J. Geophys. Res.*, 109(B11305).
513 doi: 10.1029/2003JB002932.

514 Audoine, E., Savage, K. M., Gledhill, K., 2000. Seismic anisotropy from local
515 earthquakes in the transition region from a subduction to a strike-slip plate
516 boundary, New Zealand. *J. Geophys. Res.*, 105: 8013-8033.

517 Baccheschi, P., Margheriti, L., Steckler, M. S., 2007. Seismic anisotropy reveals
518 focused mantle flow around the Calabrian slab (Southern Italy). *Geophys. Res.*
519 *Lett.*, 34. doi: 10.1029/2006GL028899.

520 Barruol, G., Granet, M., 2002. A tertiary asthenospheric flow beneath the southern
521 French Massif Central related to the west Mediterranean extension evidenced by
522 upper mantle seismic anisotropy. *Earth Planet. Sci. Lett.*, 202: 31-47.

523 Barruol, G., Deschamps, A., Coutant, O., 2004. Mapping upper mantle anisotropy
524 beneath SE France by SKS splitting indicates Neogene asthenospheric flow
525 induced by Apenninic slab roll-back and deflected by the deep Alpine roots.
526 *Tectonophysics*, 394: 125-138.

527 Battaglia, M., Murray, M. H., Serpelloni, E., Bürgmann, R., 2004. The Adriatic region:
528 an independent microplates within the Africa-Eurasia collision zone. *Geophys.*
529 *Res. Lett.*, 31, L09605. doi:10.1029/2004GL019723.

530 Bowman, J. R., Ando, M., 1987. Shear-wave splitting in the upper-mantle wedge above
531 the Tonga subduction zone. *Geophys. Jour. Roy. Astr. Soc.*, 88: 25-41.

532 Buttle, J., Olson, P., 1998. A laboratory model of subduction zone anisotropy. *Earth*
533 *Planet. Sci. Lett.*, 164: 245– 262.

534 Carminati, E., Wortel, M. J. R., Spakman, W., Sabadini, R., 1998. The role of slab
535 detachment processes in the opening of the western-central Mediterranean basins:
536 some geological and geophysical evidence. *Earth Planet. Sci. Lett.*, 160: 651-665.

537 Carminati, E., Wortel, M. J. R., Meijer, P. Th., Sabadini, R., 1998. The two-stage
538 opening of the western –central Mediterranean basins: a forward modeling test to
539 a new evolutionary model. *Earth Planet. Sci. Lett.*, 160: 667-679.

540 Chiarabba, C., Covane, L., DiStefano, R., 2005. A new view of Italian seismicity using
541 20 years of instrumental recordings. *Tectonophysics*, 395: 251-268.

542 Cimini, G. B., 1999. P-wave deep velocity structure of the Southern Tyrrhenian
543 Subduction Zone from nonlinear teleseismic travelttime tomography. *Geophys.*
544 *Res. Lett.*, 26(24): 3709-3712.

545 Civello, S., Margheriti, L., 2004. Toroidal mantle flow around the Calabrian slab (Italy)
546 from SKS splitting. *Geophys. Res. Lett.*, 31, L10601. doi:
547 10.1029/2004GL019607.

548 D'Agostino, N., Selvaggi, G., 2004. Crustal motion along the Eurasia-Nubia plate
549 boundary in the Calabrian Arc and Sicily and active extension in the Messina
550 Straits from GPS measurements. *J. Geophys. Res.*, 109(B11402). doi:
551 10.1029/2004JB002998.

552 Dewey, J. F., Helman, M. L., Turco, E., Hutton, D. W. H., Knott, S. D., 1989.
553 Kinematics of the western Mediterranean. In: M. P. Coward, D. Dietrich and R.
554 G. Park (Editors), *Alpine Tectonic. Spec. Publs geol. Soc. Lond.*, 45, pp. 265-283.

555 Faccenna, C., Piromallo, C., Crespo-Blanc, A., Jolivet, L., Rossetti, F., 2004. Lateral
556 slab deformation and the origin of the western mediterranean arcs. *Tectonics*, 23,
557 TC1012. doi: 10.1029/2002TC001488.

558 Faccenna, C., Jolivet, L., Piromallo, C., Morelli, A., 2003. Subduction and the depth of
559 convection in the Mediterranean mantle. *J. Geophys. Res.*, 108(B2), 2099.
560 doi:10.1029/2001JB001690.

561 Faccenna, C., Becker, T. W., Lucente, F. P., Jolivet, L., Rossetti, F., 2001. History of
562 subduction and back-arc extension in the Central Mediterranean. *Geophys. J. Int.*,
563 145: 809-820.

564 Faccenna, C., Civetta, L., D'Antonio, M., Funicello, F., Margheriti, L., Piromallo, C.,
565 2005. Constraints on mantle circulation around the deforming Calabrian slab.
566 *Geophys. Res. Lett.*, 32. doi: 10.1029/2004GL021874.

567 Fischer, K. M., Yang, X., 1994. Anisotropy in Kuril-Kamchatka subduction zone
568 structures. *Geophys. Res. Lett.*, 21(1): 5-8.

569 Fischer, K. M., Fouch, M. J., Wiens, D. A., Boettcher, M. S., 1998. Anisotropy and
570 flow in Pacific subduction zone back-arcs. *Pure Appl. Geophys.*, 151: 463-475.

571 Fischer, K. M., Wiens, D. A., 1996. The depth distribution of mantle anisotropy beneath
572 the Tonga subduction zone. *Earth Planet. Sci. Lett.*, 142: 253–260.

573 Fouch, M. J., Fischer, K. M., 1996. Mantle anisotropy beneath northwest Pacific
574 subduction zones. *J. Geophys. Res.*, 101(B7): 15987-16002.

575 Fouch, M. J., Fischer, K. M., 1998. Shear-wave anisotropy in the Mariana subduction
576 zones. *Geophys. Res. Lett.*, 25: 1221-1224.

577 Frepoli, A., Selvaggi, G., Chiarabba, C., Amato, A., 1996. State of stress in the
578 Southern Tyrrhenian subduction zones from fault-plane solutions. *Geophys. J.*
579 *Int.*, 125: 879-891.

580 Gledhill, K., Gubbins, D., 1996. SKS splitting and the seismic anisotropy of the mantle
581 beneath the Hikurangi Subduction Zone, New Zealand. *Physics Earth Planet.*
582 *Inter.*, 95: 227-236.

583 Gueguen, E., Doglioni, C., Fernandez, M., 1998. On the post-25 Ma geodynamic
584 evolution of the western Mediterranean. *Tectonophysics*, 298: 259-269.

585 Hatzfeld, D., Karagianni, E., Kassaras, I., Kiratzi, A., Louvari, E., Lyon-Caen, H.,
586 Makropoulos, K., Papadimitriou, P., Bock, G., Priestley, K., 2001. Shear wave

587 anisotropy in the upper mantle beneath the Aegean related to internal deformation.
588 J. Geophys. Res., 106(12): 30737–30753.

589 Hollenstein, Ch., Kahle, H-G., Geiger, A., Jenny, S., Goes, S., Giardini, D., 2003. New
590 GPS constraints on the Africa-Eurasia plate boundary zone in southern Italy.
591 Geophys. Res. Lett., 30(18). doi: 10.1029/GL017554.

592 Holtzman, B. K., Kohlstedt, D. L., Zimmerman, M. E., Heidelbach, F., Hiraga, T.,
593 Hustoft, J., 2003. Melt segregation and strain partitioning: implications for
594 seismic anisotropy and mantle flow. Science, 301: 1227-1230.

595 Jolivet, L., Faccenna, C., 2000. Mediterranean extension and the Africa-Eurasia
596 collision. Tectonics, 19: 1095-1107.

597 Jung, H., Karato, S., 2001. Water-induced fabric transitions in olivine. Science, 293:
598 1460–1463.

599 Kaminski, E., 2006. Interpretation of seismic anisotropy in terms of mantle flow when
600 melt is present. Geophys. Res. Lett., 33, L02304. doi:10.1029/2005GL024454.

601 Kaminski, E., Ribe, N. M., 2001. A kinematic model for recrystallization and texture
602 development in olivine polycrystals. Earth Planet. Sci. Lett., 189: 253–267.

603 Kaminski, E., Ribe, N. M., Browaeys, J. Y., 2004. D-Rex, a program for calculation of
604 seismic anisotropy due to crystal lattice preferred orientation in the convective
605 upper mantle. Geophys. J. Int., 158: 744–752.

606 Kincaid, C., Griffiths, R. W., 2003. Laboratory model of the thermal evolution of the
607 mantle during rollback subduction. Nature, 425: 58-62.

608 Kneller, E. A., Van Keken, P. E., Karato, S., Park, J., 2005. B-type olivine fabric in the
609 mantle wedge: insights from high-resolution non-Newtonian subduction zone
610 models. Earth Planet. Sci. Lett., 237(3-4): 781-797.

611 Levin, V., Okaya D., Park, J., 2006. Shear wave birefringence in wedge-shaped
612 anisotropic regions. *Geophys. J. Int.*, 168: 275-286.

613 Long, M. D., van der Hilst, R. D., 2005. Upper mantle anisotropy beneath Japan from
614 shear wave splitting. *Physics Earth Planet. Inter.*, 151: 206–222.

615 Long, M. D., van der Hilst, R. D., 2006. Shear wave splitting from local events beneath
616 the Ryukyu arc: trench-parallel anisotropy in the mantle wedge. *Physics Earth
617 Planet. Inter.*, 155: 300-312.

618 Lucente, F. P., Chiarabba, C., Cimini, G. B., Giardini, D., 1999. Tomographic
619 constraints on the geodynamic evolution of the Italian region. *J. Geophys. Res.*,
620 104(B9), 20: 307-20,327.

621 Lucente, P. F., Margheriti, L., Piromallo C., Barruol, G., 2006. Seismic anisotropy
622 reveals the long route of the slab through the western-central Mediterranean
623 mantle. *Earth Planet. Sci. Lett.*, 241: 517-529.

624 Lucente, P. F., Speranza, F., 2001. Belt bending driven by lateral bending of subducting
625 lithospheric slab: geophysical evidences from the Northern Apennines (Italy).
626 *Tectonophysics*, 337: 53-64.

627 Mainprice, D., Barruol, G., Ben Ismail, W., 2000. The seismic anisotropy of the Earth's
628 mantle: From single crystal to polycrystal. In: S. I. Karato (Editor), *Earth's Deep
629 Interior: Mineral Physics and Tomography From the Atomic to the Global Scale.*
630 *Geodyn. Ser.*, AGU, Washington, D. C., pp. 237-264.

631 Malinverno, A., Ryan, W. B. F., 1986. Extension on the Tyrrhenian Sea and shortening
632 in the Apennines as result of arc migration driven by sinking of the lithosphere.
633 *Tectonics*, 5: 227-145.

- 634 Margheriti, L., Lucente, F. P., Pondrelli, S., 2003. SKS splitting measurements in the
635 Apenninic-Tyrrhenian domain (Italy) and their relation with lithospheric
636 subduction and mantle convection. *J. Geophys. Res.*, 108(B4). doi:
637 10.1029/2002JB001793.
- 638 Matcham, I., Savage, M. K., Gledhill, K. R., 2000. Distribution of seismic anisotropy in
639 the subduction zone beneath the Wellington region, New Zealand. *Geophys. J. Int.*,
640 140: 1-10.
- 641 Montuori, C., Cimini, G. B., Favali, P., 2007. Teleseismic tomography of the southern
642 Tyrrhenian subduction zone: New results from seafloor and land recordings. *J.*
643 *Geophys. Res.*, 112(B03311). doi: 10.1029/2005JB004114.
- 644 Nicolosi, I., Speranza, F., Chiappini, M., 2006. Ultrafast oceanic spreading of the
645 Marsili Basin, southern Tyrrhenian Sea: Evidence from magnetic anomaly
646 analysis. *Geology*, 34(9): 717-720.
- 647 Panza, G. F., Peccerillo, A., Aoudia, A., Farina, B., 2007. Geophysical and petrological
648 modelling of the structure and composition of the crust and upper mantle in
649 complex geodynamic settings: the Tyrrhenian Sea and surroundings. *Earth-*
650 *Science Review*, 80(1-2): 1-46.
- 651 Park, J., Levin, V., 2002. Seismic anisotropy: tracing plate dynamics in the mantle.
652 *Science*, 296: 485-489.
- 653 Patacca, E., Scandone, P., 1989. Post-Tortonian mountain building in the Apennines.
654 The role of the passive sinking of a relic lithospheric slab. In: A. Boriani et al.
655 (Editors), *The Lithosphere in Italy. Atti Conv. Lincei*, 80, pp. 157-176.
- 656 Patacca, E., Sartori, R., Scandone, P., 1990. Tyrrhenian basin and Apenninic arc:
657 Kinematic relations since late Tortonian times. *Mem. Soc. Geol. It.*, 45: 425-451.

- 658 Patacca, E., Scandone, P., Tozzi, M., 2000. Il profilo CROP04. *Protecta*, 10-12: 49-52.
- 659 Pearce, J., Mittleman, D., 2002. Defining the Fresnel zone for broadband radiation.
660 *Physical Review*, E 66(5), 056602.
- 661 Peyton, V., Levin, V., Park, J., Brandon, M. T., Lees, J., Gordeev, E., Ozerov, A., 2001.
662 Mantle flow at a slab edge: seismic anisotropy in the Kamchatka region. *Geophys.*
663 *Res. Lett.*, 28: 379–382.
- 664 Piromallo, C., Morelli, A., 2003. P wave tomography of the mantle under the Alpine-
665 Mediterranean area. *J. Geophys. Res.*, 108(B2). doi: 10.1029/2002JB001757.
- 666 Plomerová, J., Arvidsson, R., Babuška, V., Granet, M., Kulhánek, O., Poupinet, G.,
667 Šílený, J., 2001. An array study of lithospheric structure across the Protogine
668 Zone, Varmland, south-central Sweden; signs of a paleocontinental collision.
669 *Tectonophysics*, 332: 1–21.
- 670 Plomerová, J., Margheriti, L., Park, J., Babuška, V., Pondrelli, S., Vecsey, L., Piccinini,
671 D., Levin, V., Baccheschi, P., Salimbeni, S., 2006. Seismic anisotropy beneath the
672 Northern Apennines (Italy): Mantle flow or Lithosphere Fabric?. *Earth Planet.*
673 *Sci. Lett.*, 247: 157-170.
- 674 Pondrelli, S., Piromallo, C., Serpelloni, E., 2004. Convergence vs. retreat in Southern
675 Tyrrhenian Sea: insights from kinematics. *Geophys. Res. Lett.*, 31, L06611.
676 doi:10.1029/2003GL019223.
- 677 Polet, J., Silver, P. G., Beck, S., Wallace, T., Zandt, G., Ruppero, R., Kind, R., Rudloff,
678 A., 2000. Shear wave anisotropy beneath the Andes from the BANJO, SEDA and
679 PISCO experiments. *J. Geophys. Res.*, 105: 6287-6304.

680 Pozgay, S. H., Wiens, D. A., Conder, J. A., Shiobara, H., Sugioka, H., 2007. Complex
681 mantle flow in the Mariana subduction system: evidence from shear wave
682 splitting. *Geophys. J. Int.*, 170: 371-386.

683 Rosenbaum, G., Lister, G. S., 2004. Neogene and Quaternary rollback evolution of the
684 Tyrrhenian Sea, the Apennines and the Sicilian Maghrebides. *Tectonics*, 23,
685 TC1013. doi: 10.1029/2003TC001518.

686 Rossetti, F., Goffè, B., Monié, P., Faccenna, C., Vignaioli, G., 2004. Alpine orogenic P-
687 T-t deformation history of the Catena Costera area and surrounding regions
688 (Calabrian Arc, Southern Italy): the nappe edifice of north Calabria revised with
689 insights on the Tyrrhenian-Apennine system formation. *Tectonics*, 23, TC6011.
690 doi: 10.1029/2003TC001560.

691 Rumpker, G., Tommasi, A., Kendall, J.-M., 1999. Numerical simulations of depth
692 dependent anisotropy and frequency-dependent wave propagation effects. *J.*
693 *Geophys. Res.*, 104(B10): 23141-23154.

694 Russo, R. M., Silver, P. G., 1994. Trench-parallel flow beneath the Nazca plate from
695 seismic anisotropy. *Science*, 263: 1105–1111.

696 Salimbeni, S., Pondrelli, S., Margheriti, L., Levin, V., Park, J., Plomerova, J., Babuska,
697 V., 2007. Abrupt change in mantle fabric across northern Apennines detected
698 using seismic anisotropy. *Geophys. Res. Lett.*, 34, L07308.
699 doi:10.1029/2007GL029302.

700 Savage, M. K., 1999. Seismic anisotropy and mantle deformation: what have we learned
701 from shear wave splitting? *Reviews of Geophysics*, 37,(1): 65-106.

702 Schmid, C., Van Der Lee, S., Giardini, D., 2004. Delay times and shear wave splitting
703 in the Mediterranean region. *Geophys. J. Int.*, 159: 275-290.

704 Selvaggi, G., 2001. Strain pattern of the Southern Tyrrhenian slab from moment tensors
705 of deep earthquakes: implications on the down-dip velocity. *Ann. Geofis*, 44: 155-
706 165.

707 Selvaggi, G., Chiarabba, C., 1995. Seismicity and P-wave velocity image of southern
708 Tyrrhenian subduction zone. *Geophys. J. Int.*, 121: 818-826.

709 Silver, P. G., 1996. Seismic anisotropy beneath the continents: probing the depth of
710 Geology. *Annu. Rev. Earth Planet. Sci.*, 24: 385-432.

711 Silver, P. G., Savage, M. K., 1994. The interpretation of shear-wave splitting parameters
712 in the presence of two anisotropic layers. *Geophys. J. Int.*, 119: 949-963.

713 Silver, P. G., Chan, W. W., 1991. Shear wave splitting and subcontinental mantle
714 deformation. *J. Geophys. Res.*, 96(B10): 16429-16454.

715 Silver, P. G., Holt, W. E., 2002. The mantle flow field beneath western North America.
716 *Science*, 295, 5557: 1054-1058.

717 Smith, G. P., Wiens, D. A., Fischer, K. M., Dorman, L. M., Webb, S. C., Hildebrand, J.
718 A., 2001. A complex pattern of mantle flow in the Lau backarc. *Science*, 292:
719 713–716.

720 Spakman, W., Van Der Lee, S., Van Der Hilst, R., 1993. Travel-time tomography of the
721 European-Mediterranean mantle down to 1400 km. *J. Geophys. Res.*, 102: 3153-
722 3166.

723 Tommasi, A., Mainprice, D., Canova, G., Chastel, Y., 2000. Viscoplastic self-consistent
724 and equilibrium-based modeling of olivine lattice preferred orientations:
725 implications for the upper mantle seismic anisotropy. *J. Geophys. Res.*, 105:
726 7893-7908.

727 Vinnik, L. P., Kind, R. 1993. Ellipticity of teleseismic S-particle motion. *Geophys.*

- 728 J. Int., 113: 165-174.
- 729 Zhang, S., Karato, S., 1995. Lattice preferred orientation of olivine aggregates deformed
730 in simple shear. *Nature*, 375: 774-777
- 731 Wortel, M. J. R., Spakman, W., 2000. Subduction and slab detachment in the
732 Mediterranean-Carpathian region. *Science*, 290: 1910-1917.
- 733

734 **Figure captions**

735 **Figure 1.** Schematic geological map of Southern Italy and Southern Tyrrhenian Sea.
736 The lines and triangles indicate the thrust front of the western Mediterranean
737 subduction zone at 16 Ma and at 0 Ma (according to *Gueguen et al. 1998*). At present
738 the subduction is active only in the Ionian domain with the Ionian oceanic lithosphere
739 dipping towards the NW beneath the Calabrian Arc. 1) main thrusts; 2) normal and
740 vertical faults; 3) fold axes; 4) Calabrian basement; 5) volcanic centers; 6a) newly-
741 formed oceanic crust; 6b) deep basins in the African-Adriatic domain; 7) African and
742 Adriatic foreland.

743 **Figure 2. a)** Hypocentral distributions of earthquakes characterizing the Southern
744 Tyrrhenian-Calabrian Arc System (*Chiarabba et al., 2005*). The different depth (in
745 km) of the events is given by the grey scale indicated on the lower left corner. The
746 distribution of events tracks the slab subducted beneath the Calabrian Arc and the
747 progressive increase of slab depth toward the central sector of the Tyrrhenian Sea, as
748 also shown by the Benioff plane isobaths (black lines). The intermediate-depth
749 earthquakes (grey circles) are confined to the front of the Tyrrhenian Calabrian coast,
750 east of the Aeolian Islands, while the deeper events are mainly concentrated offshore in
751 the Tyrrhenian Sea (black circles). **b)** Vertical sections oriented NW - SE across the
752 Ionian slab from the north sector of Calabrian arc to north-eastern sector of Sicily. The
753 lines indicate the geometry of the Tyrrhenian Moho (dashed line) and the top of the
754 Ionian slab as inferred from deep earthquakes (solid line) (*Chiarabba et al., 2005*)

755 **Figure 3.** P-wave tomography image at 150 km depth of the entire Italian Peninsula
756 and cross section of the Calabrian subduction zone (*Piromallo and Morelli, 2003*).
757 There is a well defined high velocity body, interpreted as the sinking slab, which can

758 be followed from its shallow horizontal portion, steeply dipping ($\sim 70^\circ$) toward the
759 Tyrrhenian Sea into the upper mantle and finally lying almost horizontal on the 660 km
760 discontinuity. The white solid circles are the shallow, intermediate and deep
761 earthquakes localized in correspondence with the high velocity anomaly.

762 **Figure 4.** Distribution of the epicentres of the teleseisms used in this study plotted as a
763 function of the back-azimuth and of the epicentral distance. Map location of the events.

764 **Figure 5.** Map of the 40 CAT/SCAN temporary stations used for the splitting
765 analysis. Black solid circles: stations used as examples in Figure 6. Black triangles:
766 stations at which the 90 % of seismograms are either complex and did not give a clear
767 splitting result or gave null results.

768 **Figure 6.** Examples of measurements: a null (left), a well-constrained splitting
769 measurement (centre), an analysis where we report no result (right). The upper panels
770 show four traces: the radial and transverse seismograms as recorded, and the radial and
771 transverse components after correction for the anisotropy (lower two traces). The null is
772 evident due to the absence on the transverse component of SKS energy both before and
773 after correction. For the well-constrained measurements SKS energy is clearly present
774 on the transverse trace before correction and it is removed after the correction. In the no
775 result analysis, SKS energy is clearly present on the transverse trace before and after the
776 correction for anisotropy. The time window used for the splitting analysis is shown in
777 grey. The four middle panels show the analysis window rotated in the fast (continuous
778 line) and slow (dashed line) components (uncorrected (left) and corrected (right) and
779 their respective particle motion (lower row). For the null measurement, the particle
780 motion is linear before and after the correction; for the well-determined measurement, it
781 is elliptical before and is linearized by the correction. The last panel displays the

782 contour plot of energy on the corrected transverse component showing the minimum
783 value (star symbol) of φ and δt for which the effect of stations anisotropy is best
784 removed. The stations used in those analysis are highlighted as black solid circles in
785 Figure 5.

786 **Figure 7.** Map of SKS splitting results displayed as single measurements for individual
787 station-earthquake pairs and plotted at the surface projection of the 150 km depth SKS
788 ray piercing point; this depth enable us to visually separate measurements of events
789 coming from various back-azimuths and different incidence angles. Each measurement
790 is represented as solid bars oriented in the φ direction with a length proportional to the
791 delay time, δt . Null measurements are displayed with two crossing-bars, one parallel to
792 and one normal to the back-azimuth. The thrust front is drawn as a solid black line.

793 **Figure 8.** Rose frequency plots for the three different geological domains. The trend of
794 each petal represents the azimuth φ of the fast split shear wave and the length is
795 proportional to the number of measurements in the same interval of φ (at 10° intervals)
796 weighted by the delay times of the measurements.

797 **Figure 9.** Plots of the fast directions and delay times (with their errors) versus the back-
798 azimuth of each analyzed events are presented for each of the three different domains.
799 Grey solid squares indicate the events coming from east (rays that on average sample
800 the sub-slab mantle); black solid squares indicate the events coming from west (rays
801 that on average sample the slab). Null measurements are represented by empty squares
802 and plotted as a function of back-azimuth.

803 **Figure 10.** Splitting parameters across the Southern Apennines and Apulia Platform
804 along the E-W transect from the Tyrrhenian coast to the Adriatic coast (box AA' in Fig.
805 7). φ and δt (second and third panel) are plotted as a function of the distance of the

806 stations from the Tyrrhenian coast. Black solid circles: events coming from the west
807 (back-azimuths between 0° and -180°); grey solid circles: events coming from the east
808 (back-azimuths between 0° and 180°). Open circles: null measurements. The first panel
809 shows the map location of the stations. The white line represents the thrust front. The
810 change in the fast directions between the Southern Apennines and the Apulian Platform
811 domains occurs at 120-150 km distance from the Tyrrhenian coast. The shaded area in
812 the middle panel shows the most frequent fast directions in the two domains. The third
813 panel presents the delay times versus distance.

814 **Figure 11.** Fresnel zones calculated at the stations CRAC, TRIC and ILCA close to the
815 tectonic and geological boundary between the Southern Apennines and the Apulia
816 Platform. For each station we used two teleseisms with opposite back-azimuth and we
817 have calculated the Fresnel zones radius at 50 km (white circles), 100, 150 and 200 km
818 (black circles) depth. The circles particularly overlap at 50 km depth, indicating that
819 below this depth the path of the rays differ. This suggests that the anisotropic domain is
820 below 50 km depth. The trench is drawn as solid black line.

821 **Figure 12.** Model of possible mantle flow trajectories induced by slab rollback and
822 subduction. The SKS splitting measurements at 150 km depth are shown as black bars.
823 We display the image of the slab (grey blobs) at 150 and 300 km depth, as inferred from
824 the P-waves tomography (*Piromallo and Morelli, 2003*). At 150 km depth, two slab tears
825 are evident, one below the Sicily Channel and the other one below the transition zone
826 between the Southern Apennines (S. A.) and Central Apennines (C. A.). At 300 km
827 depth, the tear below the Sicily Channel still exists, while the tear below the Southern
828 Apennines-Central Apennines is absent and the slab forms a continuous body. The large
829 black arrows indicate the mantle flow trajectories around the slab. According to the SKS

830 splitting results, mantle is hypothesized to flow around the slab, describing a ring around
831 the SW edge of the slab through the tear imaged at 150 km and 300 km depth beneath
832 the Sicily Channel. Our results do not identify such a return flow also through the tear at
833 the N-E edge of the slab, where the pattern of SKS fast directions allow us to
834 hypothesize a mantle flow parallel to the strike of the slab. The black arrows in the
835 Apulian Platform (A. P.) indicate the possible frozen in deformation not controlled by
836 the slab rollback, as deduced by the slightly not trench-parallel pattern of fast axes.

837 **Table1** - We report the complete list of 185 new individual SKS splitting parameters
838 along with the station and event parameters (Ref 1). Single measurements discussed in
839 *Civello and Margheriti, 2004* and not published elsewhere, are also included (Ref 2).

840

841

842

843

844

845

846

847

848

849

850

851

852

853

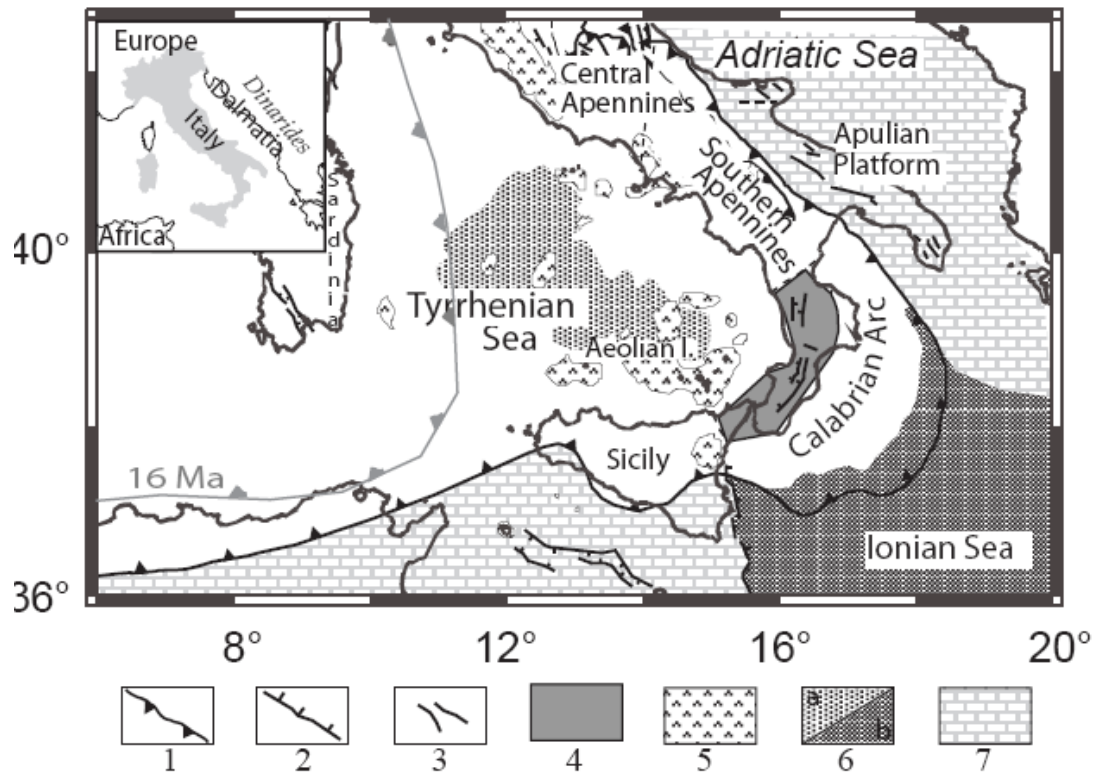


Figure 1

854

855

856

857

858

859

860

861

862

863

864

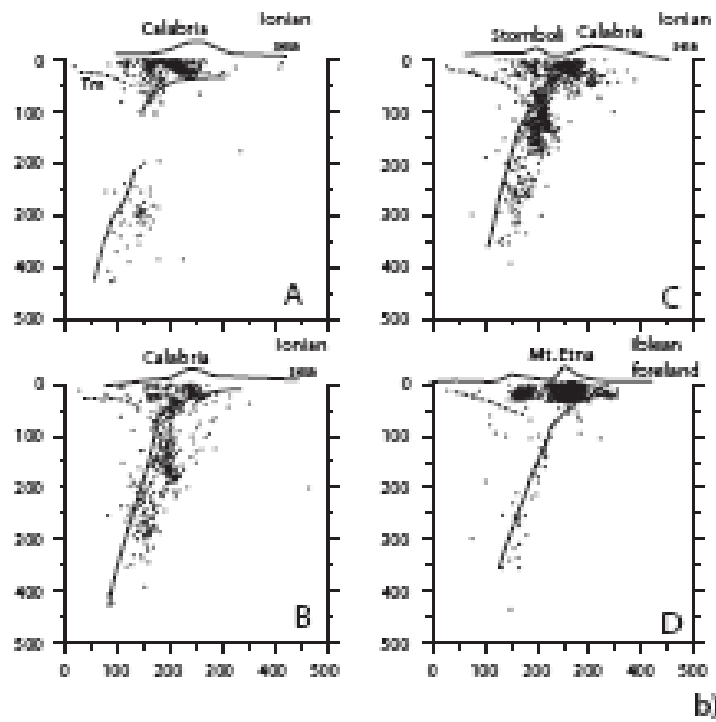
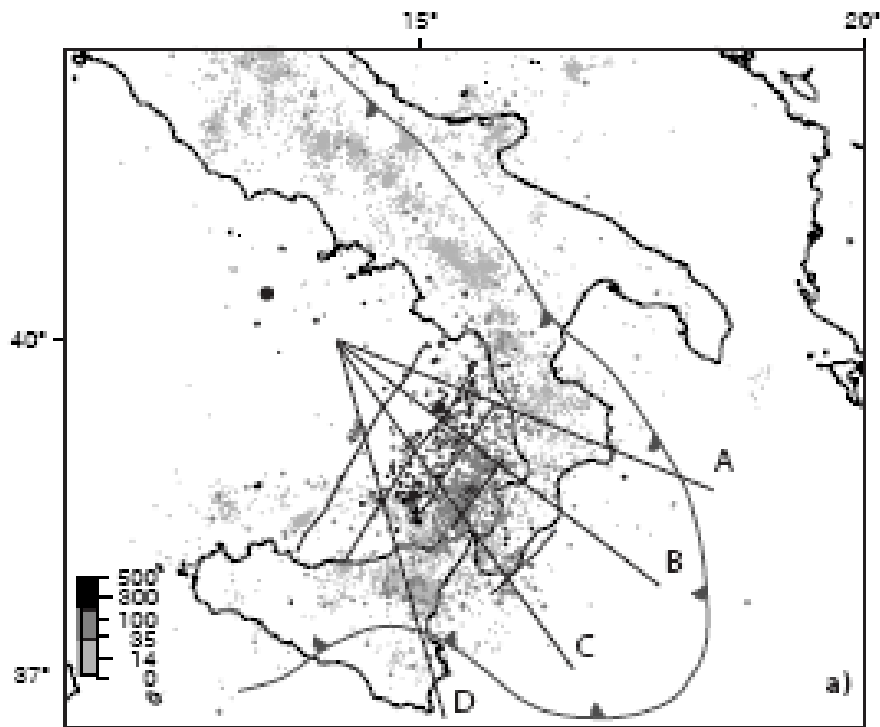


Figure 2

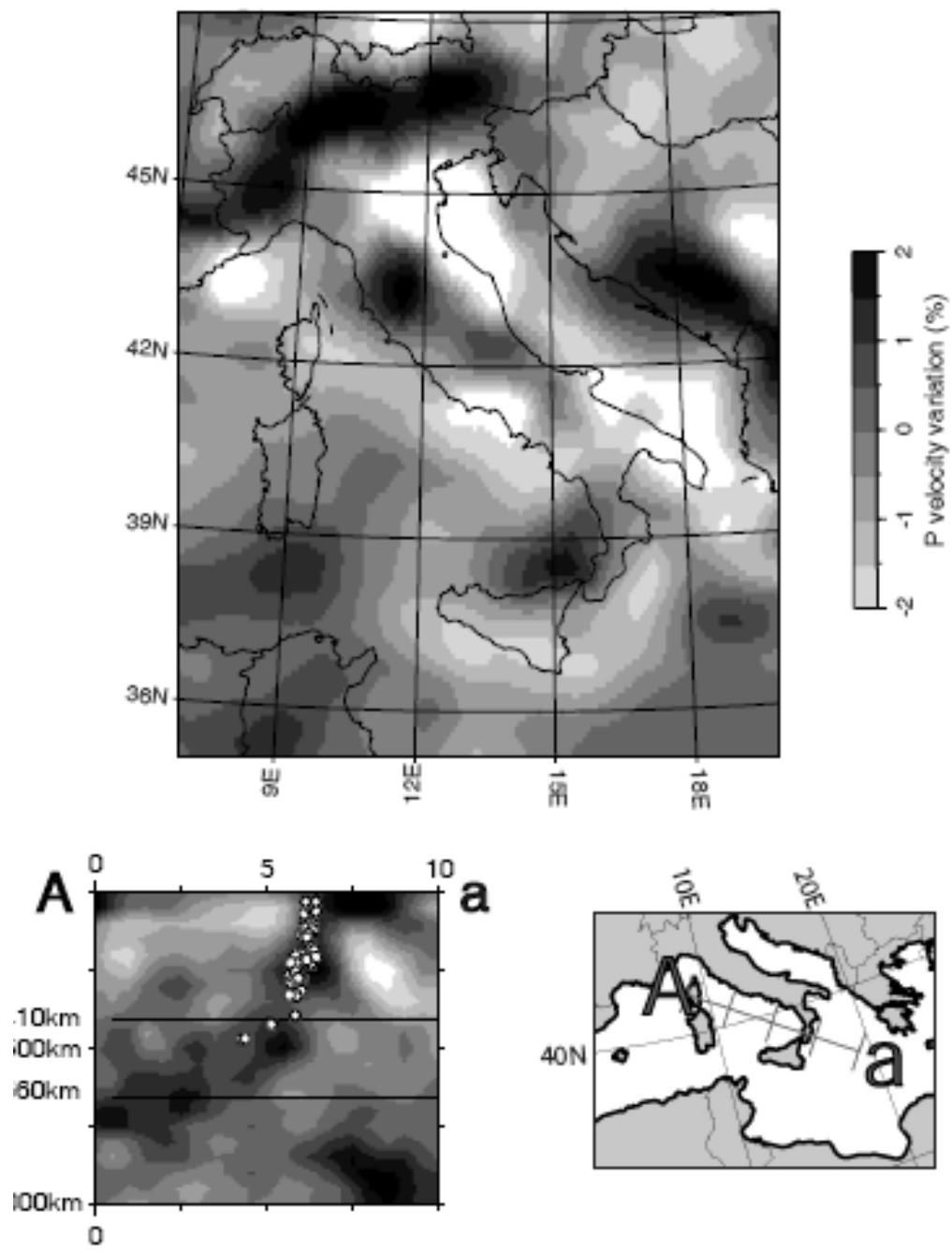


Figure 3

866

867

868

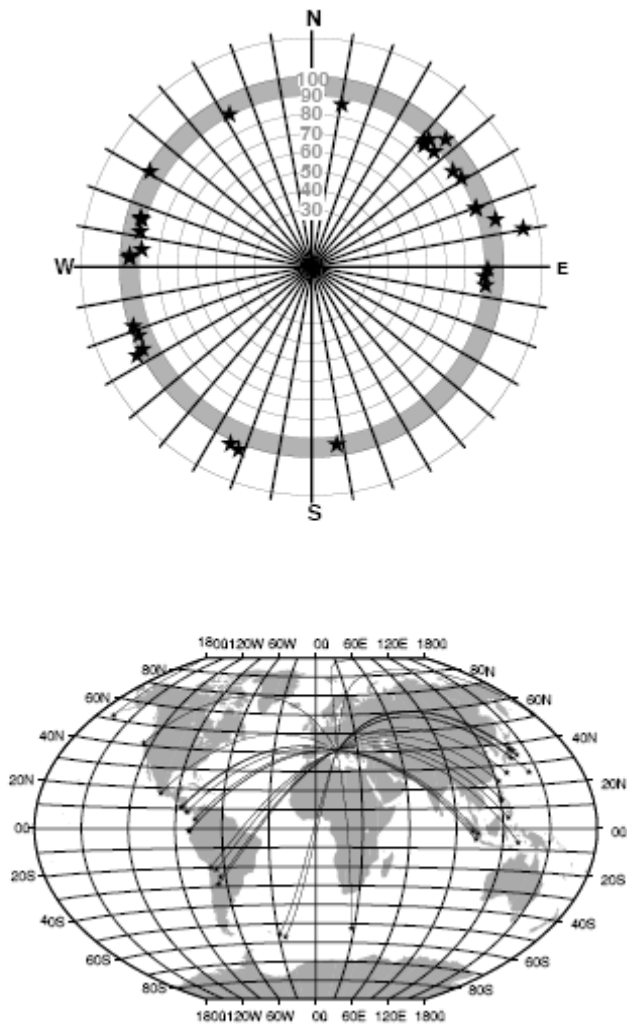


Figure 4

869

870

871

872

873

874

875

876

877

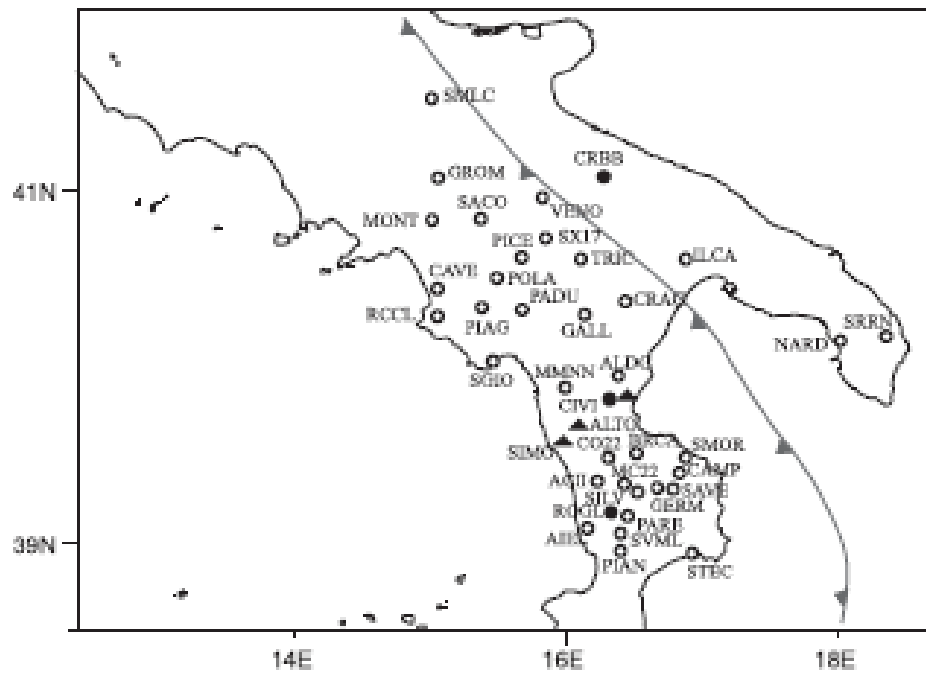


Figure 5

878

879

880

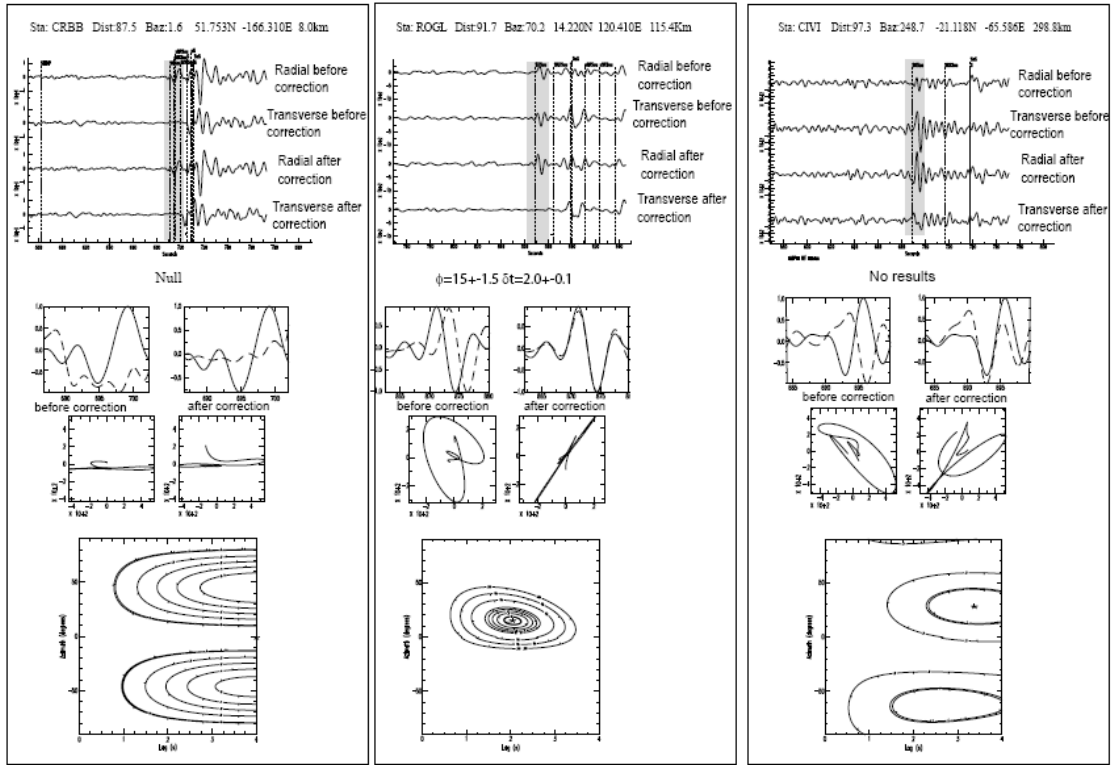


Figure 6

881

882

883

884

885

886

887

888

889

890

891

892

893

894

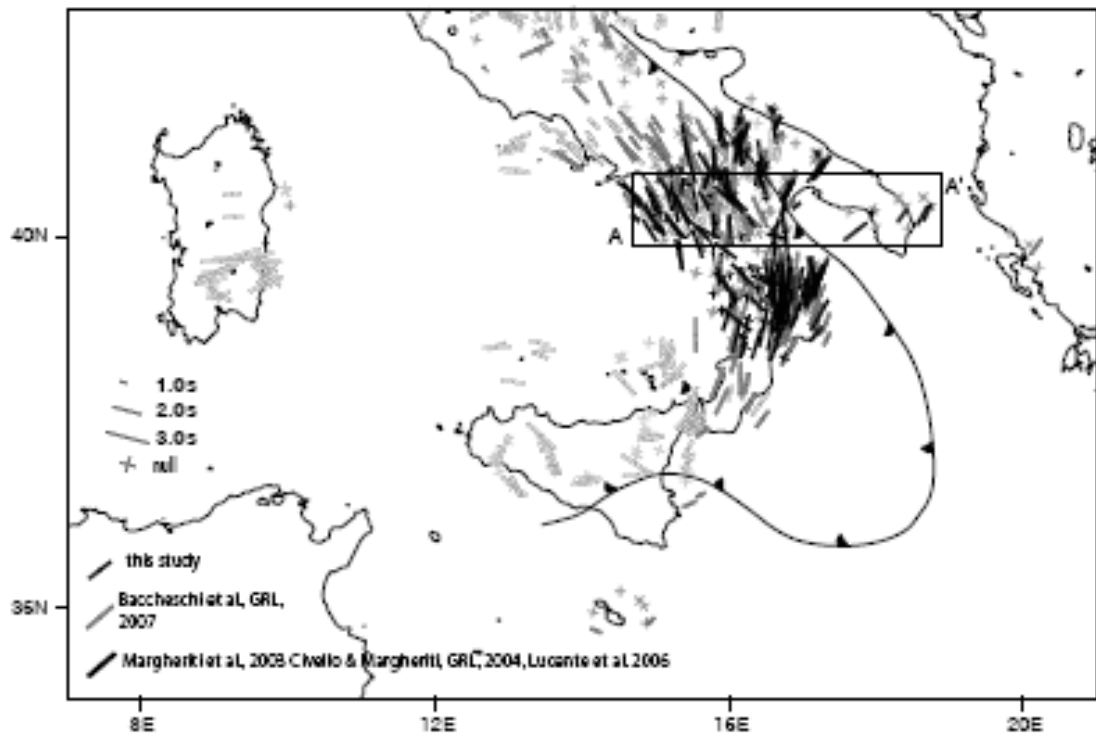


Figure 7

895

896

897

898

Southern Apennines



Apulian Platform



Calabrian Arc

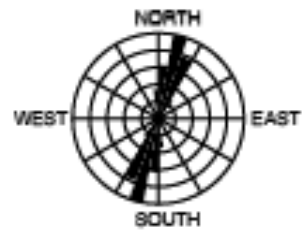


Figure 8

899

900

901

902

903

904

905

906

907

908

909

910

911

912

913

914

915

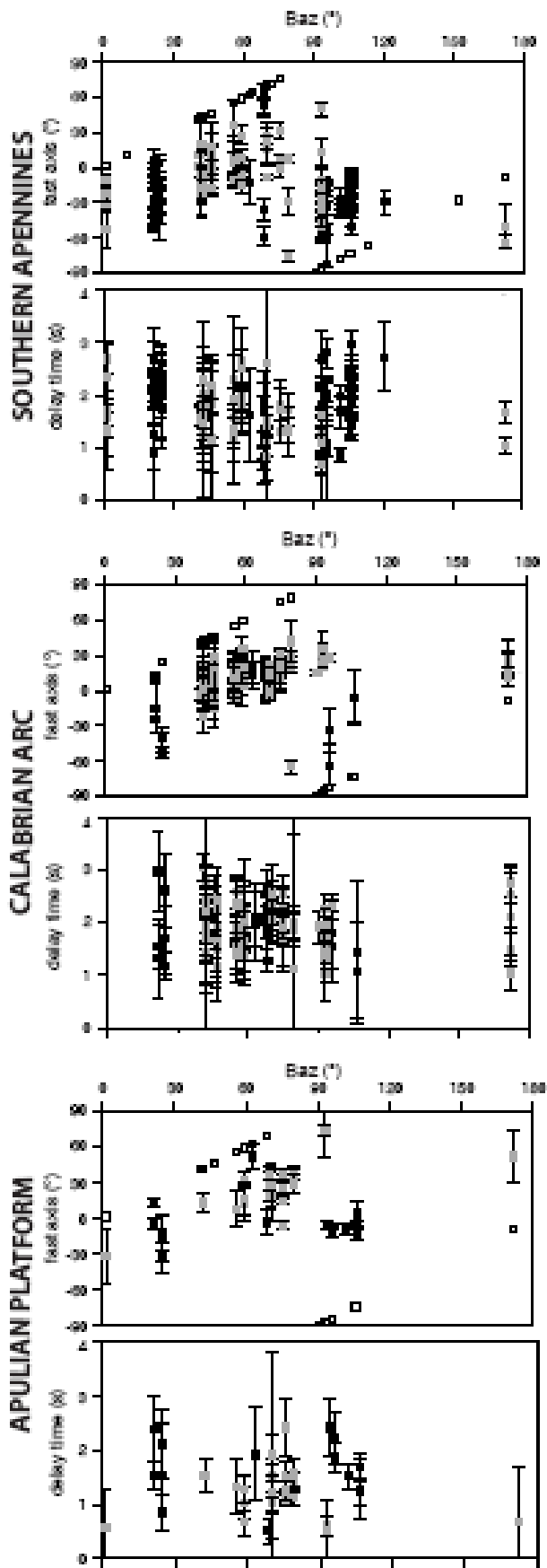


Figure 9

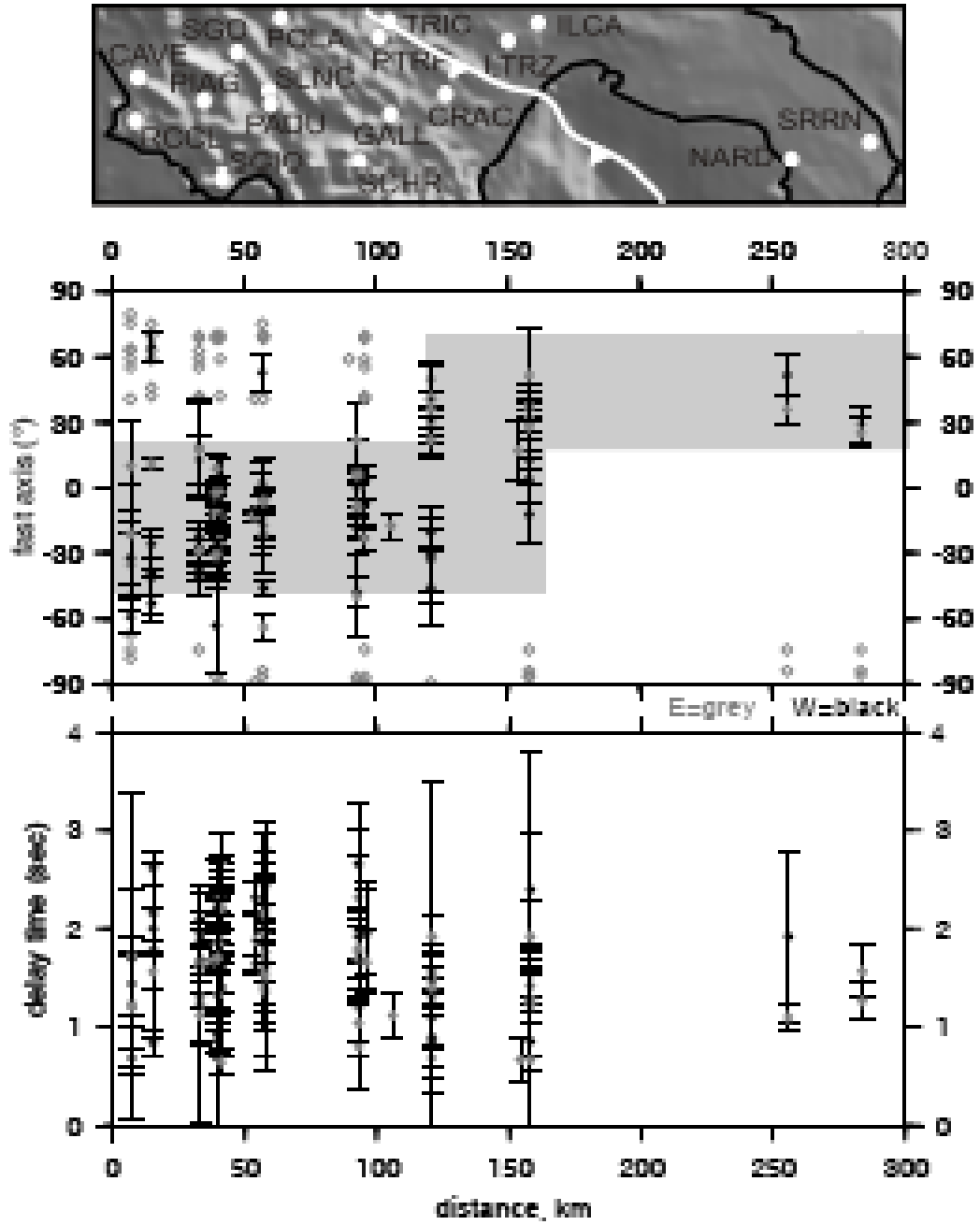


Figure 10

917

918

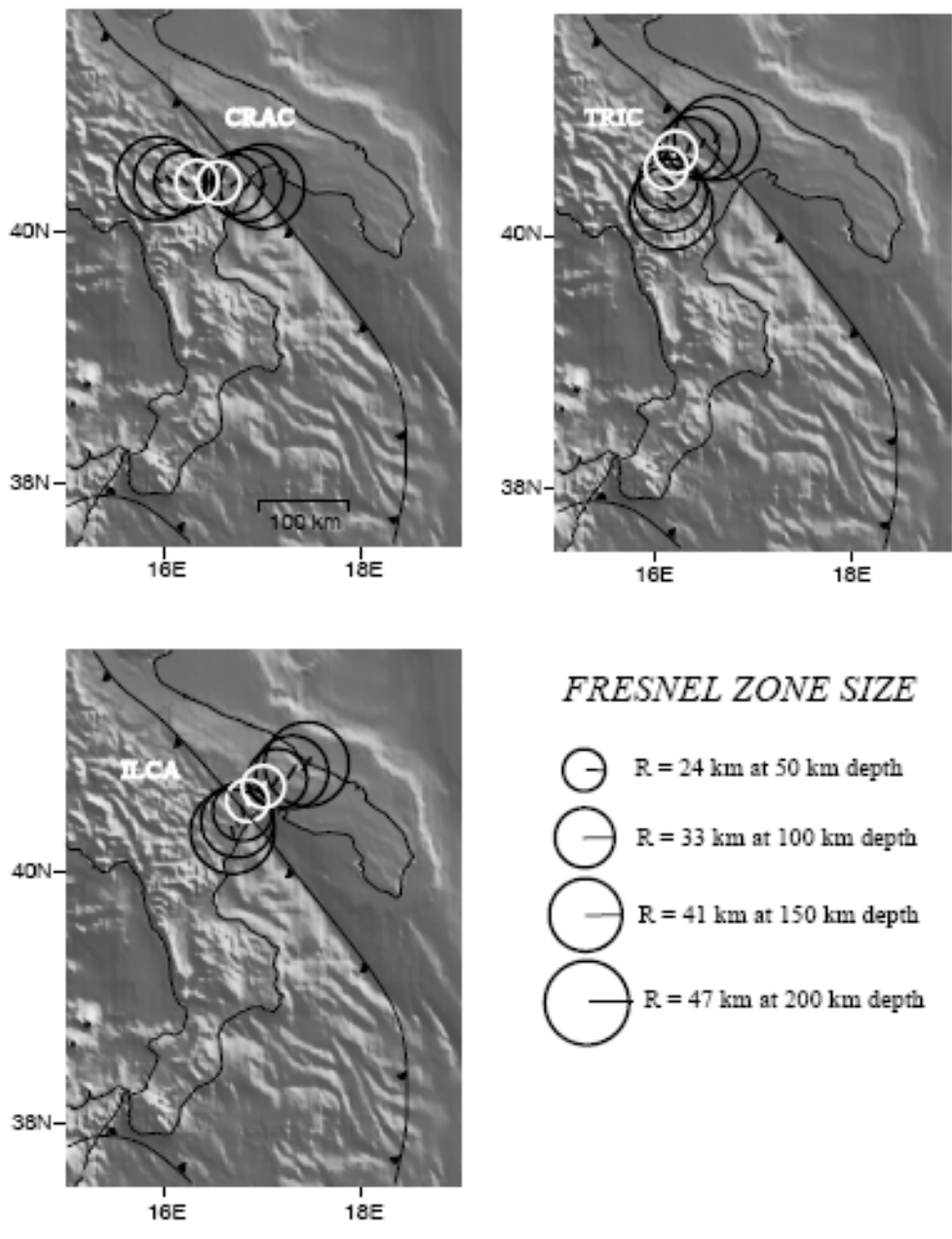


Figure 11

919
920
921
922
923

924

925

926

927

928

929

930

931

932

933

934

935

936

937

938

939

940

941

942

943

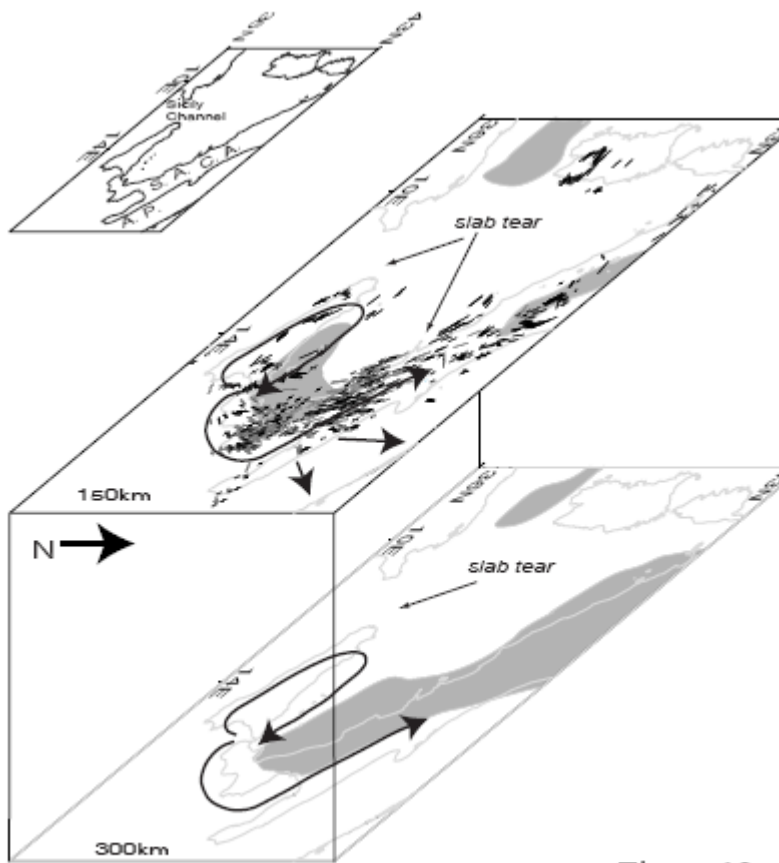


Figure 12

944

945

946